JOURNAL OF CATALYSIS 116, 1–10 (1989)

The Effect of Boron on ZSM-5 Zeolite Shape Selectivity and Activity

II. Coincorporation of Aluminium and Boron in the Zeolite Lattice

MOEIN B. SAYED,[1] ALINE AUROUX, AND JACQUES C. VÉDRINE[2]

Institut de Recherches sur la Catalyse, Laboratoire Propre du CNRS associé à l'Université Claude Bernard Lyon I, 2 Avenue Albert Einstein, 69626 Villeurbanne Cedex, France

Received July 9, 1986; revised July 25, 1988

ZSM-5 zeolite samples have been synthesized in the presence of $NaAlO_2$ and $NaBO_2$ to yield a crystalline phase of almost unchanged Al + B site population, but with increased B/Al ratio. The presence of boron in the zeolitic lattice is evident by MAS NMR. Transformation of boron (upon NH_3 sorption) within trigonal and tetrahedral symmetries, which is revealed by IR spectroscopy as persistence and disappearance of the trigonal B–O stretching mode at 1385 cm^{-1}, together with the appearance of the ≡Si—O—B= skeletal vibration at 920 cm^{-1} for the zeolite as synthesized, confirms the incorporation of boron by synthesis with no evidence of occluded amorphous boron oxide phase. IR spectroscopy reveals a distinct absorption at 3700 cm^{-1} assigned to Brønsted sites associated with lattice boron. NH_3 sorption, studied by IR spectroscopy and microcalorimetry, reveals weak acidity for boron-associated sites; however, they do certainly sorb ammonia. Kinetic data of 3-Me-pentane sorption suggest a role for lattice boron in modifying the interior part of the zeolite, which is also indicated by catalysis of toluene disproportionation as improved selectivity toward *p*-xylene formation. Zeolite modification by the present method, although exhibiting a minor effect on ZSM-5 shape selectivity, has a major role in drastically decreasing the zeolite acidity and hence activity.

INTRODUCTION

The phenomenon of shape selectivity in catalysis and sorption by zeolites has stimulated increasing interest at both the industrial and the academic levels. Substantial progress regarding modification of the zeolite shape selectivity has followed the pioneer work of Weisz and Frilette (*1*). Researchers in the decade 1970–1980 were fortunate in witnessing the birth of the most interesting shape-selective zeolite ZSM-5 (*2*). Several approaches to modifying the selectivity of this zeolite have been reported (*3–10*). At present, novel techniques appear to be promising whereby attempts are being made to replace zeolitic aluminum and/or silicon by other elements.

On the basis of the higher activity of boron than that of aluminum, it has been considered that replacing B for Al in ZSM-5 might enhance the catalytic activity. Also, as a smaller atom, boron incorporation in the zeolite framework might reduce the cell parameters and thus modify the shape selectivity. Several patents (*11–17*) have disclosed the invention of a new molecular sieve, which exhibits a structure and shape selectivity (*5*) similar to those of ZSM-5, called boralite. In boralite, B occupies a typical site of the framework Al. Catalytic activity is claimed for the new sieve (*12, 14, 18–20*), with the condition in some cases (*12, 14*) that the sieve must be pretreated in the presence of Al-based binders. Modified shape selectivity, although claimed, is not apparent. Recently, Brønsted sites of low acidity, compared with those associated with zeolite Al, have been revealed for the new sieve (*17, 21–25*). Such sites seem to be associated with B, since counterpart sites are not evident for the typically structured silicalite sieve.

[1] Present address: Chemistry Department, Faculty of Science, Al-Azhar University, Cairo, Egypt.

[2] To whom correspondence should be addressed.

0021-9517/89 $3.00

In a different approach, Derouane *et al.* (*26*) have chosen to modify ZSM-5 by B incorporation in an already synthesized zeolite. The data of their study have revealed a linear decrease in catalytic activity with modification, i.e., with the decreased Al content being replaced by boron.

The aim of the present investigation has been to study the effect of increased boron (at the expense of lattice aluminum) populations on both catalytic activity and shape selectivity of ZSM-5 and to compare such an effect of B incorporation with that of B impregnation (*27*).

EXPERIMENTAL

Materials

High-purity-grade methanol and toluene (Merck) were used as reactants for both catalytic methanol conversion and xylene formation. Dried (over Na wire) and degassed (by freeze–pump–thaw cycles) ammonia was used to probe modified zeolite acidity, the key to modified catalytic activity.

Zeolite Modification

The modified zeolite was synthesized according to example 1 of Ref. (*2*), with a precaution to avoid contaminating the reaction with CO_2 as previously described (*28*). In addition to the original H–ZSM_0-5, several samples were synthesized with the intention of incorporating boron at an increased population so that the product would exhibit an increased B/Al ratio, with B + Al being almost unchanged. This has been followed by adding $NaAlO_2$ (alone or mixed with $NaBO_2$) to colloidal silica in tetrapropylammonium hydroxide. The resultant milky solution was homogenized by gentle warming prior to subjecting the assembly to freeze–pump–thaw cycles. The Pyrex vessel used for the reaction was then sealed and placed in a steel bomb which was heated in a furnace at 423 K for a period of 1 week. The crystalline cake was filtered, crushed, washed several times with distilled water, and then dried at 393 K.

The crystalline phase was identified as of ZSM-5 structure by both X-ray diffraction (*29*) and infrared band absorbance ratio (*30*), A_{550}/A_{450} of ca. 0.61 (Table 2). The acidic samples were obtained from their parent derivatives by acid ion exchange in 0.5 *M* HCl at 353 K/6 h. The results of elemental analysis are reported in terms of sites per zeolite unit cell (Table 1).

Sorption Measurements

Both the capacity and the kinetics of *n*-hexane and 3-Me-pentane sorption (P/P_s = 0.1) were studied by thermogravimetry with a Sartorius microbalance at 293 K for samples outgassed (0.1 mPa) at 673 K/12 h.

Acidity Measurements

(*i*) *Infrared spectroscopy.* Zeolite samples (ca. 14 mg) were pressed (5700 kPa) into thin wafers (5 mg cm^{-2}). The IR spectra (200–4000 cm^{-1}) were recorded with 2.8 cm^{-1} resolution, using a double-beam Perkin–Elmer Series 580 spectrometer. Highly absorbing lattice vibrations were measured using the KBr disk (2% dilution) technique. NH_3 at a pressure of 1.33 kPa was admitted at 373 K onto wafers outgassed (0.1 mPa) at 673 K/2 h. Physisorbed NH_3 was pumped off at 293 K, as indicated by the IR spectrum. Other spectral measurements were performed following NH_3 desorption at 373 K and higher temperatures.

(*ii*) *Microcalorimetry.* The heat of NH_3 sorption was studied by introducing succes-

TABLE 1

Zeolite Elemental Analysis "in Terms of Site per Unit Cell"

Zeolite	Symbol	Si	Al	B	Na	Al + B	B/Al
H–ZSM_0-5	○	91.8	4.1	0.1	0.5	4.2	0.02
H–ZSM_1-5	△	91.1	4.0	0.9	0.6	4.9	0.23
H–ZSM_2-5	□	91.2	3.2	1.6	1.0	4.8	0.50
H–ZSM_3-5	▼	91.9	2.8	1.3	0.9	4.1	0.47
H–ZSM_4-5	⬡	91.7	2.6	1.7	0.6	4.3	0.65

TABLE 2

Data from IR Spectroscopy, Hydrocarbon Sorption at 293 K (P/P_0 = 0.1), and SEM

Zeolite	IR A_{550}/A_{450}	Wt% sorption		Crystal size (μm)
		3-Me-pentane	*n*-Hexane	
H–ZSM$_0$-5	0.61	7.1	11.5	0.8–1.5
H–ZSM$_1$-5	0.62	7.1	11.5	0.5–0.7
H–ZSM$_2$-5	0.62	6.8	11.1	0.5–0.7
H–ZSM$_3$-5	0.61	6.7	10.5	2.0–5.0
H–ZSM$_4$-5	0.59	6.8	11.1	0.5–0.8

sive small doses (0.04 cm^3) onto the zeolite (100 mg) at 423 K as previously described (*31*). Both volumetric and calorimetric data were collected at elevated pressures (ca. 0.013 to 133 Pa), using a Setaram Tian-Calvet microcalorimeter equipped with a Datametric Barocel gauge of 133 Pa pressure range and computer microprocessing.

Catalytic Activity and Shape Selectivity Measurements

A fixed amount of the zeolite (50 mg) was activated under N_2 at 673 K/14 h and was then used for either toluene/CH_3OH (4/1) alkylation (WHSV = 5 h^{-1}) or toluene disproportionation (WHSV = 0.5 h^{-1}) at 673 K as previously described (*27*). Catalytic activity was measured as toluene conversion as a function of time, while shape selectivity was measured as mole percent *p*-xylene formed with respect to other isomers.

RESULTS AND DISCUSSION

Sorption of Hydrocarbons Studied by Thermogravimetry

Sorption of *n*-hexane and 3-Me-pentane has been performed at 293 K. The maximum sorption capacity measured after 16 h of sorption is reported in Table 2. Both adsorbates show either comparable or slightly lowered (with increased boron content) capacities, relative to those reported for ordinary (*32*) ZSM-5. It is interesting to point out that, while the sorption kinetics (Fig. 1) of 3-Me-pentane are almost unaffected at early sorption stages, a progressive decrease is revealed with increased boron content at later stages. This may reflect a role of boron in slightly constraining the interior part of the zeolite, provided both morphology and size of crystallites are similar (Table 2, column 5) except for H–ZSM$_3$-5 exhibiting larger crystallite size.

The State and Acidity of Boron as Studied by Infrared Spectroscopy

One of the most important features to investigate by infrared spectroscopy is to identify whether the skeleton Si–O–B is formed during the zeolite synthesis or not. Figure 2a shows the IR spectrum of H–ZSM-5 as synthesized, i.e., as Na, TPA–ZSM$_2$-5. The spectrum is dominated by absorptions associated with occluded TPA vibrations (*3*). In the lower region of the spectrum two distinct absorptions appear at 920 and 670 cm^{-1} exclusively for the modi-

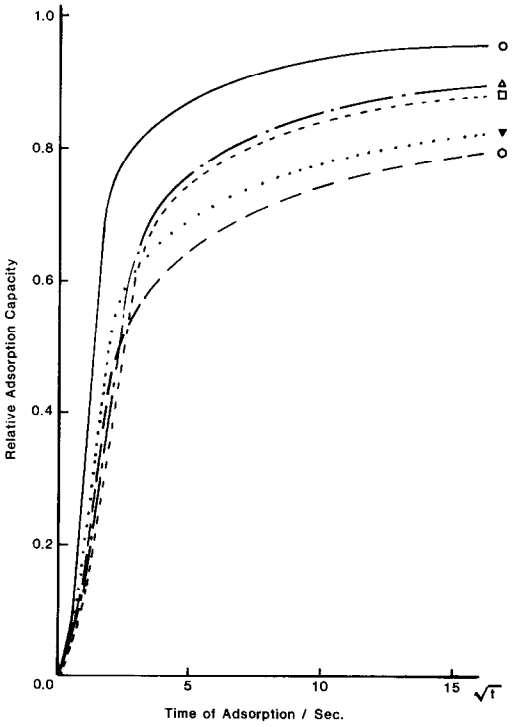

FIG. 1. Dependence of sorption kinetics of 3-Me-pentane on zeolite boron content. For symbol significance in this and later figures, see Table 1.

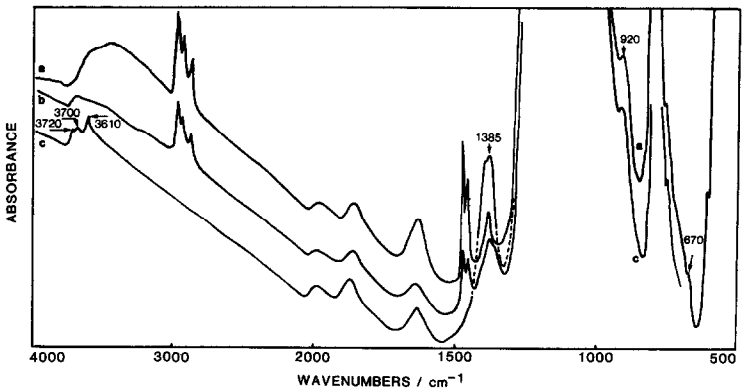

FIG. 2. Infrared spectra of Na, TPA–ZSM_2-5. (a) Spectrum of the zeolite as synthesized; (b) same as for (a), but after pretreatment at 0.1 mPa/673 K for 6 h; (c) same as for (b), but after further pretreatment at 723 K for 4 h.

fied samples, where they intensify with increased (Fig. 3) boron content. Such absorptions are observed for borosilicates and are assigned to skeletal, Si–O–B (*33*) vibrations. TPA^+ cations decompose partly (Fig. 2b) upon outgassing the sample (0.1 mPa) at 673 K/6 h, with the appearance of a broad band at 1385 cm^{-1} which is progressively developed with increased TPA^+ decomposition (Fig. 2c). Moreover, the band intensity of that mode increases with the zeolite boron content, which indicates association with boron (see Fig. 3). The absorption at 1385 cm^{-1} is very sensitive to sorption of basic sorbates, where it diminishes upon NH_3 sorption (Fig. 4b) with the appearance of a band characteristic of NH_4^+ at 1460 cm^{-1}. This is reversible (Fig. 4c) with the sorbate desorption. The same phenomenon is detected upon hydration of borosilicate films (*3*) and upon sorption of NH_3, CH_3OH, and H_2O onto pure boralite samples (*22*) (see Scheme 1).

Since it is evident that the 1385 cm^{-1} ab-

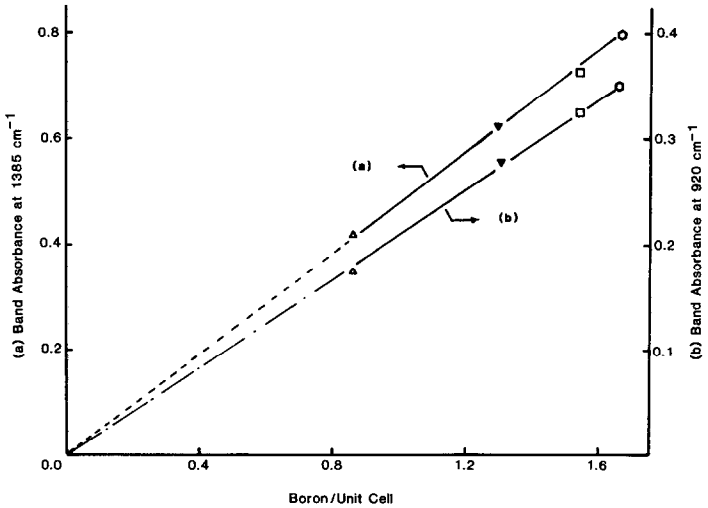

FIG. 3. Variation of IR band intensity with the zeolite boron content. (a) At 1385 cm^{-1}; (b) at 920 cm^{-1}.

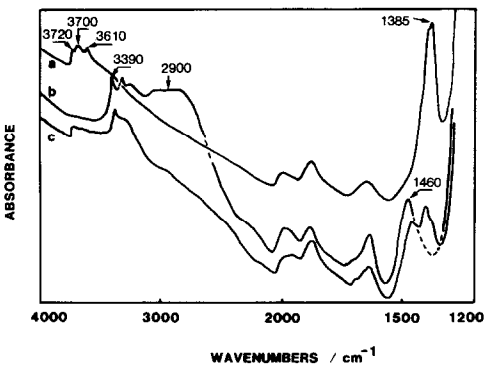

FIG. 4. Infrared spectra of H–ZSM$_4$-5. (a) Zeolite pretreatment at 673 K for 2 h; (b) same as for (a), but after NH_3 sorption at 373 K; (c) same as for (b), but after desorption for 15 min at 293 K.

sorption appears only when the zeolite is present in the protonic form, it may then be suggested that the electron affinity for protons is so great that coordination of the lone pair electrons at lattice oxygen to boron Lewis sites does not favorably occur. Replacing H^+ by a cation of less electron affinity, e.g., NH_4^+, allows such coordination to take place leading to structure II (*23, 24*). It appears therefore that boron in structure I occupies a trigonal site which transforms to a tetrahedral site upon sorption of basic sorbates (structure II). Thus, it is appropriate to assign the absorption at 1385 cm^{-1} to a trigonal B–O stretching vibration (*34, 35*). The disappearance of that absorption upon NH_3 sorption and recovery upon NH_3 desorption are consistent with the reversible site transformation (structure I $\rightleftarrows$ structure II), since the tetrahedral B–O stretching mode absorbs infrared radiation at lower frequencies which could not be identified because of the highly absorbing tetrahedral Si–O stretch near this spectral region.

In the spectral region appreciably above 3000 cm^{-1}, three absorptions appear at 3720, 3700, and 3610 cm^{-1} (Figs. 2 and 4) and are assigned to nonacidic surface SiO–H, boron-associated Brønsted sites, and Al-associated Brønsted sites respectively. B-associated Brønsted sites absorbing at 3700 cm^{-1} have already been reported (*23–25*), and Al-associated Brønsted sites absorbing at 3610 cm^{-1} are well known (*37*). Table 3 reveals the ideal association of the absorbance at 3610 cm^{-1} with Al-associated Brønsted site population, H^+_{Al}. The higher wavenumber, distinguishing weak absorption of B-associated Brønsted sites, would indicate a higher SiO–H bond force constant, which suggests lower acidity than that of Al-associated Brønsted sites.

Modified Acidity as Studied by Microcalorimetry (38)

Previous reports (*22–24*) on boralite samples have shown quite a weak acidity for boron-associated acid sites. Measurable acidity has been detected only for samples contaminated with aluminium. In the present investigation, Table 4 reports sorption capacities collected from sorption isotherms given in Ref. (*38*) at 0.5 and 1.0 Torr for samples pretreated at 673 and 1073 K. As shown, both B and Al sites contribute equally to sorption capacity, where ideal correlation of the moles of NH_3 sorbed with the total acid site population (Table 3) is

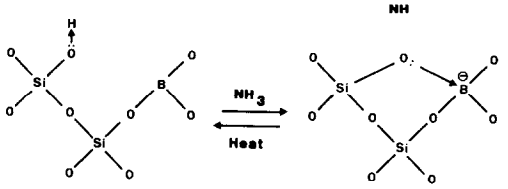

SCHEME 1

TABLE 3

Data from Elemental and IR Analyses "in Terms of Site per Unit Cell"

Zeolite	H^+_{total}	H^+_{Al}	$A_{3610\ cm^{-1}}$
H–ZSM$_0$-5	3.7	3.6	0.100
H–ZSM$_1$-5	4.3	3.4	0.095
H–ZSM$_2$-5	3.8	2.2	0.085
H–ZSM$_3$-5	3.2	1.9	0.055
H–ZSM$_4$-5	3.7	2.0	0.060

Note. H^+_{total} = (Al + B) − Na and H^+_{Al} = Al − Na.

TABLE 4

Sorption and Thermal Data Calculated from NH_3 Sorption at 423 K for Samples Degassed at 673 and 1073 K in Moles per Unit Cell (*38*)

Zeolite	Pretreated at 673 K			Pretreated at 1073 K		
	Average sites		Strong sites	Average sites		Strong sites
	0.5 Torr	1 Torr		0.5 Torr	1 Torr	
H–ZSM_0-5	4.8	5.3	2.0	3.6	3.9	1.6
H–ZSM_1-5	5.2	5.9	1.4	4.0	4.4	1.3
H–ZSM_2-5	5.0	5.7	1.1	3.8	4.1	0.8
H–ZSM_3-5	4.1	4.7	0.8	3.1	3.5	0.4
H–ZSM_4-5	4.5	5.0	0.9	2.9	3.4	0.5

revealed. This is true for either Brønsted (673 K) or Lewis (1073 K) acid sites. At variance, only Al-associated acid sites (Table 3, H^+_{Al}) contribute to the zeolite strong acidity that evolves heat of ca. 150 ± 10 kJ mol^{-1}. Following a method based on a thermokinetic parameter (*21*), only the number of strong acid sites could be precisely calculated. The ideal correlation associating zeolite strong acidity to lattice aluminum holds true for either Brønsted sites (Table 4, column 4) or Lewis sites (Table 4, column 7); compare the order of strength with Al site population (Table 3). This would clearly indicate that boron-associated acid sites (Brønsted or Lewis), although sorbing NH_3, do not release measurable heat, which suggests weak acidity.

Calorimetric measurement at 423 K has been very important in differentiating surface acidity into order of strength, and hence distinguishes homogeneous and heterogeneous distributions. Homogeneous acidity distribution can be viewed in the differential heat as an abrupt change with surface coverage, which indicates interaction with only two types of strong and weak sites. When NH_3 neutralizes all the strong sites revealing an upper level heat plateau, the differential heat drops to a lower level heat plateau corresponding to the weak sites. Heterogeneous acidity distribution, on the other hand, is viewed as a systematic decrease in the differential heat with coverage indicating interaction with sites of varying strength. Figure 5 in Ref. (*38*) shows the differential heat for samples outgassed at 673 K. As shown, the more the zeolite is modified the more heterogeneously are acid sites distributed. Surface heterogeneity increases in the order H–ZSM_2-5 > H–ZSM_4-5 > H–ZSM_3-5 > H–ZSM_1-5 > H–ZSM_0-5. A typical order is shown in Fig. 6 of Ref. (*38*) for samples outgassed at 1073 K. This would indicate that a portion of the strong sites associated with aluminum is re-

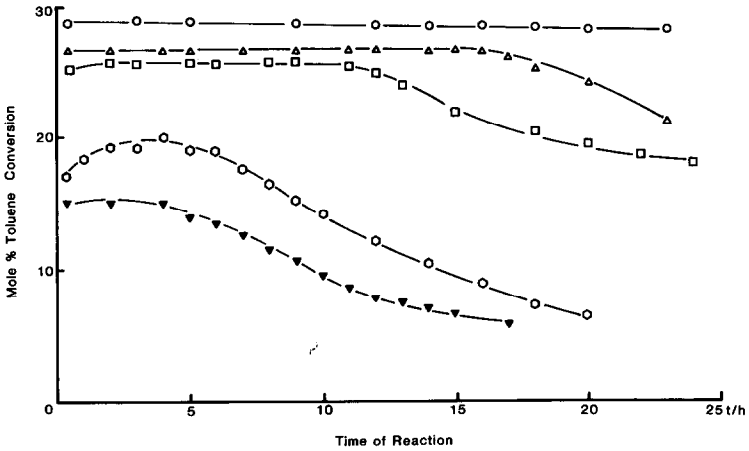

FIG. 5. Activity sequence and decay with time on stream for toluene/CH_3OH alkylation (WHSV of 5 h^{-1} at 673 K) for samples pretreated under N_2 at 673 K for 14 h.

TABLE 5

Toluene/CH_3OH Alkylation, Mole Percent Product Distribution at 1 h

Mol%	Zeolite				
	H–ZSM_0-5	H–ZSM_1-5	H–ZSM_2-5	H–ZSM_3-5	H–ZSM_4-5
C_1–C_2	0.8	1.5	1.1	1.5	1.7
Xylenes	84.0	75.6	77.9	82.5	80.9
C_8	15.2	22.9	21.0	16.0	17.4
o-Xylene	14.0	18.1	18.7	11.6	14.0
m-Xylene	25.6	32.8	31.3	16.0	31.5
p-Xylene	60.4	49.1	50.0	72.4	54.5

placed by a weaker one associated with boron. This is applicable for either Brønsted sites or Lewis sites (*38*).

Catalytic Studies

(*i*) *Toluene alkylation by methanol.* The data of alkylation (Fig. 5) indicate clearly that catalytic activity follows a typical order of zeolite strong acidity for samples activated at 673 K. While H–ZSM_0-5 exhibits a catalytic activity which is maintained high with reaction on stream, other modified samples exhibit lower activity decreasing for the more modified sample. This would exclude any function for boron, whereas Al-associated Brønsted sites, H^+_{Al} (Table 3), are the sole zeolite centers contributing to catalytic activity. Zeolite shape selectivity may be identified in terms of the less bulky *p*-xylene formed in the catalytic process, with respect to other xylene isomers. Table 5 shows the product distribution of that process (WHSV = 5 h^{-1} at 673 K) at high activity levels. As reported, the formation of xylenes is the dominant process with percentages of 80 ± 5 over all the samples. The amount of *p*-xylene formed over H–ZSM_3-5 is exceptionally high and cannot be claimed to zeolite modification with boron, since a higher boron-incorporating sample, H–ZSM_2-5 or H–ZSM_4-5 (Table 1), shows a lower selectivity (Table 5). The modified shape selectivity shown for H–ZSM_3-5 can be a consequence of larger particle size (2–5 μm) (*39*) than that exhibited by other samples (Table 2, column 5).

At variance with the distinct modified shape selectivity shown by impregnated zeolite samples (*27*), a similar effect is not revealed in the present investigation. Furthermore, strange phenomena associated with boron mobility for the impregnated samples (*27*) are not detected in the present case. These would confirm boron incorporation in the zeolite lattice and exclude possible occlusion of an amorphous boron oxide phase for the present modification. Experimental data from X-ray diffraction (*23, 39*) and MAS NMR (*24*) confirm the suggestion of boron incorporation in the zeolitic lattice. The distinct NMR signal at ca. −3 ppm, which characterizes tetrahedral boron (*16*), is revealed for all the samples exhibiting boron intensity correlating with the zeolite boron content. Other signals indicative of other boron phases are not detected. In addition to the good crystallinity indicated by the IR A_{550}/A_{450} band absorbance ratio and intense X-ray patterns, evidence of boron incorporation can be established by such techniques only with difficulty, due to the canceling effect of aluminum on the unit cell parameters, which may be effected by the larger Al atom.

(*ii*) *Toluene disproportionation.* Because of its mechanism involving bimolecular intermediates (*27*), toluene disproportionation was employed to probe possible shape selectivity modification with boron. The data of disproportionation (Fig. 6) for samples activated at 673 K (WHSV = 0.5 h^{-1} at 673 K) reveal almost stable activity on

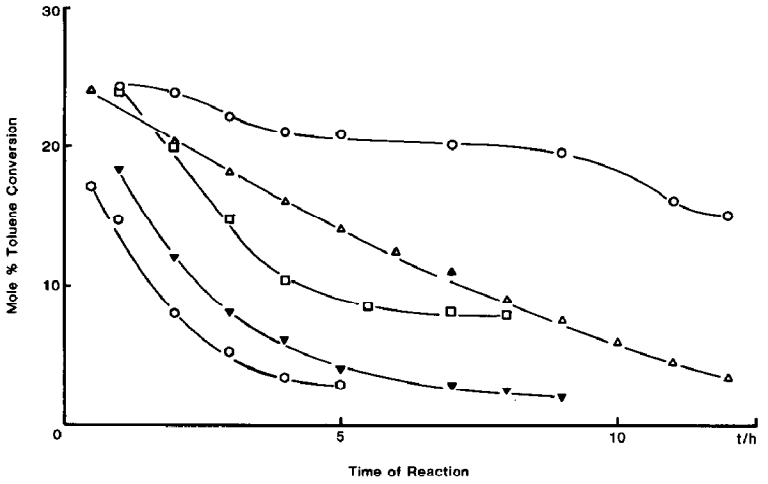

FIG. 6. Activity and decay with time on stream for toluene disproportionation (WHSV of 0.5 h^{-1} ; 673 K) for samples pretreated under N_2 at 673 K for 14 h.

stream for H–ZSM_0-5; however, the lifetime of the catalyst is shorter than that for alkylation (Fig. 5). Zeolite deactivation increases in an order following the rise in the B/Al (Table 2) ratio. Boron functions (side by side) with the lowered H^+_{Al} population in decreasing disproportionation activity, which is at variance with alkylation having no role for boron. This could suggest a role for boron in modifying the interior section of the zeolite, which could find supporting evidence from sorption data (see Fig. 1 and Table 2). Table 6 reports the data regarding shape selectivity. As expected, toluene disproportionation yields equal proportions of benzene and xylene, the latter dominated by the *m*-isomer. As revealed by alkylation for H–ZSM_3-5, *p*-xylene forms in e tionally high proportion (Table 6) for sample, and to a lesser extent for H–Z 5. Modified shape selectivity can main a consequence of crystal size (*39*) and lesser extent a boron effect. The concl that boron represents not only a weak site but also a constraint in the interio of the zeolite so that it retards catalys the processes involving bulky inter ates can be drawn.

CONCLUSION

Against expectations based on the fundamental chemistry of the elem which favors boron over aluminum more active element, the results of inc

TABLE 6

Toluene Disproportionation, Mole Percent Product Distribution at 1 h

Mol%	Zeolite				
	H–ZSM_0-5	H–ZSM_1-5	H–ZSM_2-5	H–ZSM_3-5	H–Z
Benzene	45.4	43.0	49.0	47.1	4
Xylenes	54.2	56.0	50.4	52.3	4
o-Xylene	22.0	24.0	23.0	16.8	1
m-Xylene	65.0	62.0	63.0	42.6	5
p-Xylene	13.0	14.0	14.0	40.6	2
C_8	0.4	1.0	0.6	0.6	

rating boron into the zeolite structure reveal clearly lower activity. For instance, boron in BF_3 is a stronger Lewis acid than aluminum for AlF_3. This basic rule is not further applied to oxides, particularly those of zeolitic nature. While alumina is known as a solid of strong Lewis acidity, boria is not useful in that respect. Moreover, aluminosilicates exhibit surfaces of strong Brønsted and Lewis acidities, which is at variance with borosilicates having no considerable acidity. This fact is further explicit in the present investigation. Such unusual low acidity associated with boron in oxides contributes to low catalytic activity and short lifetime. Over these disadvantages zeolite shape selectivity is not really modified by boron incorporation in the zeolitic structure. This is probably due to the presence of aluminum, which exerts an opposite effect on the unit cell parameters. Unit cell shrinkage effected by boron might be canceled by the larger atom, aluminum.

ACKNOWLEDGMENTS

The synthesis of the modified zeolite samples has been performed at the Chemistry Department of the University of Newcastle, N.S.W., Australia. One of the authors (M.B.S.) is very grateful to Professor R.P. Cooney of the University of Newcastle for his continuous encouragement toward this project; he is also indebted to CNRS, France, for the generous support which allowed such a project to be fruitfully carried out.

REFERENCES

1. Weisz, P. B., and Frilette, V. J., *J. Phys. Chem.* **64,** 382 (1960).
2. Argauer, R. J., and Landolt, G. R., U.S. Patent 3,702,886 (1972).
3. Chu, C. C., U.S. Patent 3,965,210 (1976).
4. Butter, S. A., and Kaeding, W. W., U.S. Patent 3,965,209 (1976).
5. Butter, S. A., U.S. Patents 3,979,472 (1976) and 4,007,231 (1977).
6. Kaeding, W. W., Chu, C. C., Young, L. B., Weinstein, B., and Butter, S. A., *J. Catal.* **67,** 159 (1981).
7. Kaeding, W. W., Chu, C. C., Young, L. B., and Butter, S. A., *J. Catal.* **69,** 392 (1981).
8. Young, L. B., Butter, S. A., and Kaeding, W. W., *J. Catal.* **76,** 418 (1982).
9. Védrine, J. C., Auroux, A., Dejaifve, P., Ducarme, V., Hoser, H., and Zhou, S. B., *J. Catal.* **73,** 147 (1982).
10. Derouane, E. G., Dejaifve, P., Gabelica, Z., and Védrine, J. C., *Faraday Discuss. Chem. Soc.* **72,** 331 (1982).
11. Taramasso, M., Manara, G., Fattore, V., and Notari, B., French Patent 2,429,182 (1980).
12. Klotz, M. R., U.S. Patents 4,268,420, 4,285,919, 4,292,457 (1981).
13. Barrer, R. M., "Hydrothermal Chemistry of Zeolites," p. 251. Academic Press, London/New York, 1982.
14. Kutz, N. A., *in* "Proceedings, 2nd Symp. of Industry University Cooperative Chem. Program," p. 121. Texas A & M Univ. Press, College Station, TX, 1984.
15. Dessau, R. M., and Kerr, G. T., *Zeolites* **4,** 315 (1984).
16. Gabelica, Z., Debras, G., and B. Nagy, J., "Catalysis on the Energy Scene" (S. Kaliaguine and A. Mackay, Eds.), Stud. Surf. Sci. Catal. Series, Vol. 23, p. 113. Elsevier, Amsterdam, 1984.
17. Chu, C. T. W., and Chang, C. D., *J. Phys. Chem.* **89,** 1569 (1985).
18. Holderich, N., Eichorn, H., Lehnert, R., Marosi, L., Mross, W., Reinke, R., Ruppel, W., and Schlimper, H., *in* "Proceedings, VIth Intern. Conf. on Zeolites, Reno, 1983" (D. Olson and A. Bisio, Eds.), p. 545. Butterworths, London, 1984.
19. Borade, R. B., Halgeri, A. B., and Prasad Rao, T. S. R., *in* "Proceedings, VIIth Intern. Conf. on Zeolites" (Y. Murakami, A. Iijima, and J. W. Ward, Eds.), p. 581. Elsevier, Amsterdam, 1986.
20. Beyer, M. K., and Borbely, G., *in* "Proceedings, VIIth Intern. Conf. on Zeolites" (Y. Murakami, A. Iijima, and J. W. Ward, Eds.) p. 867. Elsevier, Amsterdam, 1986.
21. Auroux, A., Sayed, M. B., and Védrine, J. C., *Thermochim. Acta* **93,** 557 (1985).
22. Auroux, A., Coudurier, G., Shannon, R., and Védrine J. C., *in* "Proceedings, AFCAT Meeting, Montpellier, 1985" (S. Partyka, and M. Lindheimer, Eds.), Vol. 16, p. 68, 1985.
23. Coudurier, G., and Védrine, J. C., *Pure Appl. Chem.* **58,** 1389 (1986).
24. Coudurier, G., Auroux, A., Védrine, J. C., Farlee, R. D., Abrams, L., and Shannon, R. D., *J. Catal.* **101,** 1 (1987).
25. Scholle, K. F., Kentgens, A. P. M., Veeman, W. S., Frenken, P., and van der Valden, G. P., *J. Phys. Chem.* **88,** 5 (1984).
26. Derouane, E. G., Baltusis, L., Dessau, R. M., and Shmitt, K. D., "Catalysis by Acids and Bases" (B. Imelik, *et al.*, Eds.), Stud. Surf. Sci. Catal. Series, Vol. 20, p. 135. Elsevier, Amsterdam, 1985.

27. Sayed, M. B., and Védrine, J. C., *J. Catal.* **101,** 43 (1986).
28. Sayed, M. B., and Cooney, R. P., *Aust. J. Chem.* **135,** 2483 (1982).
29. Wu, E. L., Lawton, S. L., Olson, D. H., Rohrman, A. C., and Kokotailo, G. T., *J. Phys. Chem.* **83,** 2777 (1979).
30. Coudurier, G., Naccache, C., and Védrine, J. C., *J. Chem. Soc. Chem. Commun.,* 1413 (1982).
31. Auroux, A., Védrine, J. C., and Gravelle, P. C., "Adsorption at the Gas–Solid and Liquid–Solid Interfaces" (J. Rouquerol, and K. S. W. Sing, Eds.) Stud. Surf. Sci. Catal. Series, Vol. 10, p. 305. Elsevier, Amsterdam, 1982.
32. Chen, N. Y., and Garwood, W. E., *J. Catal.* **52,** 453 (1978).
33. Sayed, M. B., Kydd, R. A., and Cooney, R. P., *J. Catal.* **88,** 137 (1984).
34. Tenney, A. S., and Wong, J., *J. Chem. Phys.* **56,** 5516 (1972).
35. Wong, J., *J. Electrochem. Soc.* **127,** 62 (1980).
36. Taft, E. A., *J. Electrochem. Soc.* **118,** 1985 (1971).
37. Védrine, J. C., Auroux, A., Bolis, V., Dejaifve, P., Naccache, C., Wierzchowski, P., Derouane, E. G., Nagy, J. B., Gilson, J.-P., van Hooff, J. H. C., van den Berg, J. P., and Wolthuizen, J., *J. Catal.* **59,** 248 (1979).
38. Sayed, M. B., *Thermochim. Acta* **126,** 325 (1988).
39. Védrine, J. C., Coudurier, G., and Mentzen, B. F. "Perspectives in Molecular Sieve Science" (W. H. Flank and T. E. Whyte, Eds.), A.C.S. Symp. Ser., Vol. 368, p. 66. Amer. Chem. Soc., Washington, DC, 1988.